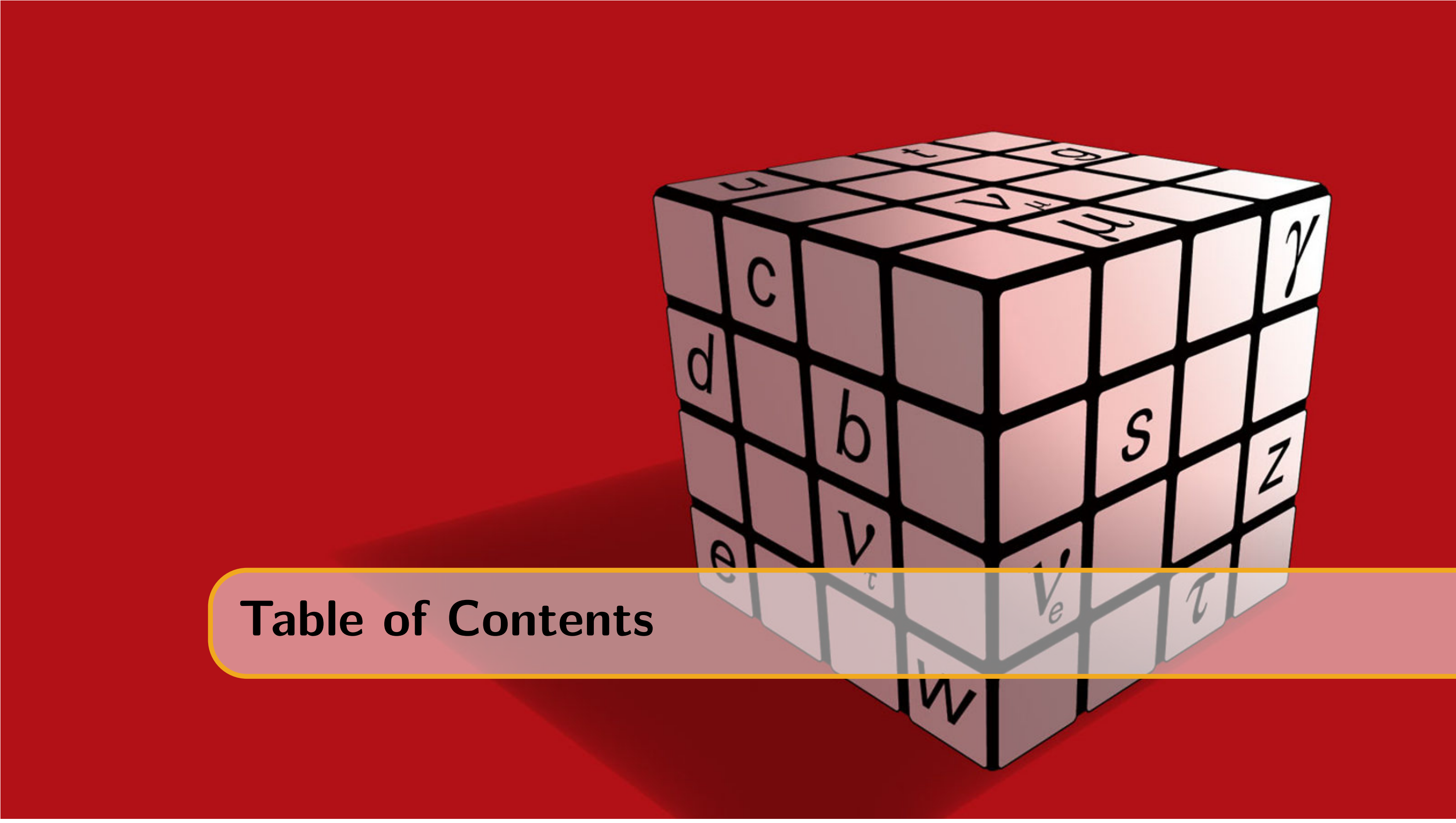

Table of Contents

I	Theory and Experiment

II	Simulation, Processing and Analysis

1	**Simulation: Event Generation and Propagation**	**7**
1.1	**Generation**	**8**
1.1.1	Background simulation	8
1.1.2	Signal simulation	10
1.2	**Propagation**	**10**
1.2.1	PROPOSAL	12
1.2.2	Photoelectron generators	13
1.3	**Data processing**	**14**
1.4	**Weighting**	**14**
2	**Reconstruction and ???**	**15**
2.1	**IceHive**	**15**
2.2	**Line-Fit**	**15**
2.3	**SPE and MPE**	**15**
2.4	**Millipede**	**15**
2.5	**Boosted Decision Tree Classifiers**	**15**
3	**The SPACE Analysis**	**17**
3.1	**Motivation**	**17**
3.2	**General strategy**	**17**
3.3	**Event cleaning**	**17**
3.4	**Variables**	**17**
3.5	**BDT results**	**17**

3.6 Pull validation 17
3.7 Systematic Uncertainties 17
3.8 Results 17

4 Summary and Discussion 19

Appendices 21

A Gauge symmetries 23

B Planck's law 25
B.1 Electromagnetic waves in a cubical cavity 25
B.1.1 Classical approach 26
B.1.2 Quantum approach 26

C Statistics 27

D Distributions 29
D.1 Spherical random numbers 29
D.2 Power law distributions 31
D.3 Angular distributions 31

Bibliography 33

Index 43

Theory and Experiment

II

Simulation, Processing and Analysis

1 Simulation: Event Generation and Propagation 7
1.1 Generation
1.2 Propagation
1.3 Data processing
1.4 Weighting

2 Reconstruction and ??? 15
2.1 IceHive
2.2 Line-Fit
2.3 SPE and MPE
2.4 Millipede
2.5 Boosted Decision Tree Classifiers

3 The SPACE Analysis 17
3.1 Motivation
3.2 General strategy
3.3 Event cleaning
3.4 Variables
3.5 BDT results
3.6 Pull validation
3.7 Systematic Uncertainties
3.8 Results

4 Summary and Discussion 19

Appendices 21

A Gauge symmetries 23

B Planck's law 25
B.1 Electromagnetic waves in a cubical cavity

C Statistics 27

D Distributions 29
D.1 Spherical random numbers
D.2 Power law distributions
D.3 Angular distributions

Bibliography 33

Index 43

1. Simulation: Event Generation and Propagation

In order to be able to search for new physics, one has to have a good handle on the detector response on known physics events. Depending on the analysis, some processes are more interesting than others. In general, the particle interactions of interest are referred to as *signal events*. Other interactions, which mimic or obscure the signal events, are typically called *background events*. These events are simulated using Monte Carlo[*] (MC) simulations, where one makes use of a model that describes the interactions and their probability to occur. A typical MC simulation consists of hundreds to millions of events that are constructed using these models from random number generators. To determine the detector response of a particle interaction, one first has to start with the particle generation, which defines the properties of the interaction. Afterwards, the propagation of the particle in the detector (medium) is simulated as best as possible. Below, we give an overview of the important background and signal simulations that are used in this analysis.

> **Corollary 1.0.1 — The software framework.** is a modular framework written and used by the IceCube collaboration and mostly written in C++ for fast computation. A python interface for most modules is provided for fast and easy implementation of the code. The framework is used in both online and offline processing. The framework is stream-based with modules that act on events in the stream and is essentially follows the flowchart that is provided by the user.
>
> To process the large amount of simulation that is required for the collaboration, a data processing and management framework called *IceProd* was developed. The setup is very light-weight, running as a python application. It uses (complex) workflow DAGs (see below) across distributed computing grids in order to optimize usage of resources. A *dataset* is set up by running hunders to thousands of jobs in parallel over multiple computing resources all over the world. Each dataset has specific input parameters that are fixed. Distributions in physical parameters such as the direction, energy, position, etc. of the particle(s) are privided by random number generators [135].

[*] While recovering from an illness in 1946, Stanislaw Ulam figured that the actual counting of succesful attempts in playing a card game would yield him a much faster answer to the probability of succes rather than doing the actual calculus. His work, shared with John von Neumann, needed to remain secret and adopted the code word , referring the gambling games in the Monte Carlo Casino in Monaco.

> *HTCondor* is an open source computing software that provides a job queueing mechanism, scheduling policy, priority scheme, resource monitoring, and resource management. Users submit their serial or parallel jobs to HTCondor, HTCondor places them into a queue, chooses when and where to run the jobs based upon a policy, carefully monitors their progress, and ultimately informs the user upon completion.
>
> *DAGMans* (Directed Acyclic Graph Managers) are meta-schudulers for the execution of computations. They submit the programs to HTCondor in an order that is represented by a DAG and processes the results. DAGMans are often used by analyzers for bulk computations on large amounts of data.

1.1 Generation

Simulations start with setting up the starting conditions of the physical processes one wants to simulate. For example, a shower event by itself is not well defined. The type of primary particle (H, He, Fe,...), the energy, the inclination and so on will all define the properties of the air shower that will be produced. Multiple different generators used in the IceCube collaboration serve other purposes; some are explained in more detail below.

1.1.1 Background simulation

1.1.1.1 CORSIKA

A free, publicly available software framework that is widely used in the astrophysics community for the simulation of cosmic ray interactions is called (COsmic Ray SImulations for Kascade). It was originally developed for the KASCADE experiment and now used by most people and collaborations to simulate air shower events. In-ice analyses, such as this one, use CORSIKA simulations to simulate the muonic component that is able to reach the in-ice detector.

A particle of specific type, energy, direction and position is injected in the top of the atmosphere and propagated. The distribution of particles in the shower is saved and read out at a certain altitude. Because the flux of cosmic rays is exceedingly small at the highest energies, too many resources and too much time would be required to simulate an energy distribution as measured in experiments. Therefore, one often simulates a much harder spectrum and reweights the events accordingly later on (see Section 1.4). Simulation datasets are often subdivided into a low-energy and high-energy dataset. The former ranges from primary energies between 600 GeV to 100 TeV and uses a spectral index that is close to what is measured. The spectral index of the latter is smaller, resulting in a harder spectrum, and the primary energy ranges from 100 TeV to 100 EeV. The lower limit of the energy range is due to the limited penetration depth of muons through the ice. An overview is given in Table 1.2.

The spectrum used for this analysis, after reweighting, follows the following energy distribution:

$$\Phi_i\left(E_{\text{prim}}\right) = \sum_{j=1}^{3} a_{i,j} E^{-\gamma_{i,j}} \cdot \exp\left[-\frac{E}{Z_i R_{c,j}}\right]. \tag{1.1}$$

where we sum over the three populations that are mentioned in Section **??**, γ is the spectral index, Z the particle atomic number and $a_{i,j}$ the normalization constants for primary i in population j. The 5 groups that are assumed to contribute significantly to the flux are: p, He, CNO, Mg-Si and Fe. This is the convention that is used in Ref. [93]. Table 1.1 shows the best fits for the normalization constants to describe the data.

Interactions

The atmosphere composition is always set at 78.1% N_2, 21% O_2, and 0.9% Ar, which is a good description of reality. However, the density of the air above the detector changes significantly

Table 1.1: Best fit for parameters in Eq. 1.1. Numbers taken from Ref. [93]

j	R_c [V]	γ					$a_{i,j}$				
		p	He	CNO	Mg-Si	Fe	p	He	CNO	Mg-Si	Fe
1	$4 \cdot 10^{15}$	1.66	1.58	1.63	1.67	1.63	7860	3550	2200	1430	2120
2	$30 \cdot 10^{15}$	1.4					20		13.4		
3	$2 \cdot 10^{18}$	1.4					1.7		1.14		

during the year because of temperature differences in the Arctic Summer and Winter. Most analyses that treat the muonic component as a background and are not interested in the details of the showers and how it's changes during the year use an average of the atmospheric density.

The shower propagation and composition depends on the models that are used to simulate these high-energy interactions. The lowest energies are simulated with (FLUktuierende KAskade) [136]. This model covers the energy range that can be compared with accelerator experiments. Which model is the best for the highest energies is not known at the time of writing, if there even is one, since there are no controlled laboratory measurements that are capable of reaching these energies. Several studies seem to indicate that the composition changes drastically at the highest energies [**SAMCITEREN+andere**]. Fortunately, this is of no large importance for this analysis.

is written in FORTRAN 77, but a C++ version is currently in the making [137].

1.1.1.2 NuGen

The is a neutrino event generator program that works with the IceTray framework (see Section ???). With this module, one can inject a primary neutrino on the surface of the Earth by specifying a few parameters in the steering file.

The physics implemented in this program is based on the ANIS-All Neutrino Interaction Generator [138]. However, the cross sections have been updated and the structure of code has been changed significantly from ANIS to incorporate it in the framework.

The generator requires the first interaction to be near the detector and

- prepares a primary neutrino and injects it to the Earth,
- propagates the neutrino and makes interactions inside the Earth (if it happens),
- makes a forced interaction inside the detection volume (only if any neutrino reaches the detector site),
- stores injected neutrinos and all generated secondaries
- stores interaction weight information

Since the generators forces the interaction to occur (to optimize computational resources), the interaction weight has to take this into accound.

The generator also does not distinguish between neutrino and antineutrino and assumes a ratio of (1:1).

The spectrum used for this analysis, after reweighting, follows the Honda2006 spectrum [124] for atmospheric neutrinos, SarcevicStd for the prompt component [127], and astrophysical from [139]. The astrophysical flux measured by the IceCube collaboration follows the following energy spectrum

$$E^2 (\Phi) = 1.5 \cdot 10^{-8} \left(\frac{E}{100 \text{ TeV}} \right)^{-0.3} \text{GeV cm}^{-2}\text{s}^{-1}\text{sr}^{-1} \tag{1.2}$$

The distribution for these different components can be seen in Fig. **??**.

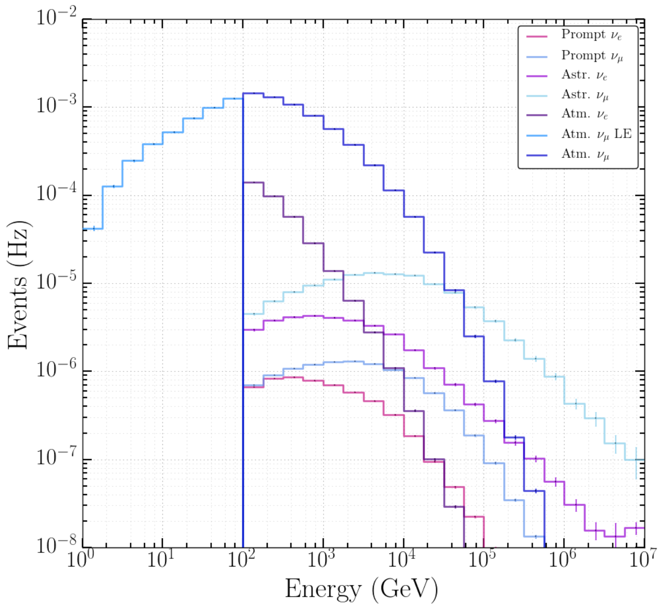

Figure 1.1: Distribution of weighted neutrino fluxed that were used for this analysis. The atmospheric ν_μ and ν_e fluxes were derived from Ref. [124], prompt from Ref. [127], and astrophysical from Ref. [139].

1.1.1.3 GENIE

To include the lowest energies, which are not accounted for by ANIS/NuGen, the GENIE (Generates Events for Neutrino Interaction Experiments) neutrino generator was implemented in IceTray. It is a well established generator, used by collaborations worldwide and written in C++ [140, 141].

The spectrum used for this analysis, after reweighting, follows the Honda2015 spectrum [**Honda:2015fna**] for low-energy atmospheric neutrinos.

1.1.2 Signal simulation

As mentioned in Section **??**, the signal is assumed to be isotropic close to the detector. The SMP starting points are randomly placed on a disk with a direction perpendicular to it as shown in Fig. 1.2 below. The disk has a radius of 800 m and is located at a distance of 1000 m from the detector center. The disk itself is randomly rotated around the detector center to simulate an isotropic flux. The distribution of the azimuth, ϕ and cosine of the zenith*, $\cos\theta$, is shown in Fig. 1.3.

Because slow moving particles would require specific treatment, the minimal velocity of the particles is set as $\beta > 0.95$ and simulated with a E^{-1} spectrum. The spectrum is later normalized a flux of 10^{-14} GeV cm^{-2}s^{-1}sr^{-1} with an E^{-2} spectrum. The absolute flux is only necessary for illustrative purposes, see Section ???.

Similar to the background, SpiceLea was used as the nominal ice model.

1.2 Propagation

After generation, the particles need to be propagated through the medium. The particles will interact, lose energy, produce new particles, and generate light. The particle interactions and light production are done in two different modules as photon simulation is done with GPU. The former module is called *PROPOSAL*, the latter *ppc*.

*See Appendix D.3 why we show the cosine of the zenith.

Table 1.2: Overview of the datasets used in this analysis. GaisserH3a from Ref. [93], Honda2015 from Ref. [**Honda:2015fna**], Honda2006 from Ref. [124], Sarcevic from Ref. [127], and astrophysical from Ref. [139]

Generator	Type	Range [GeV]	Simulated γ	Weighted γ	Ice	Dataset
CORSIKA	HE 5-comp.	$10^5 - 10^{11}$	2	GaisserH3a	SpiceLea	11937
CORSIKA	LE 5-comp.	$600 - 10^5$	2.6	GaisserH3a	SpiceLea	11499
CORSIKA	LE 5-comp.	$600 - 10^5$	2.6	GaisserH3a	SpiceLea	11808
CORSIKA	LE 5-comp.	$600 - 10^5$	2.6	GaisserH3a	SpiceLea	11865
CORSIKA	LE 5-comp.	$600 - 10^5$	2.6	GaisserH3a	SpiceLea	11905
CORSIKA	LE 5-comp.	$600 - 10^5$	2.6	GaisserH3a	SpiceLea	11926
CORSIKA	LE 5-comp.	$600 - 10^5$	2.6	GaisserH3a	SpiceLea	11943
CORSIKA	LE 5-comp.	$600 - 10^5$	2.6	GaisserH3a	SpiceLea	12161
CORSIKA	LE 5-comp.	$600 - 10^5$	2.6	GaisserH3a	SpiceLea	12268
GENIE	ν_μ	$0.5 - 100$	1	Honda2015	SpiceMie	12475
NuGen	ν_μ	$100 - 10^8$	2	atmos.: Honda2006 prompt: Sarcevic astro.: Astro.	SpiceLea	11029
NuGen	ν_μ	$100 - 10^8$	2	atmos.: Honda2006 prompt: Sarcevic astro.: Astro.	SpiceLea	12346
NuGen	ν_μ	$100 - 10^8$	2	atmos.: Honda2006 prompt: Sarcevic astro.: Astro.	SpiceLea	11883
NuGen	ν_e	$100 - 10^8$	2	atmos.: Honda2006 prompt: Sarcevic astro.: Astro.	SpiceLea	12034
NuGen	ν_e	$100 - 10^8$	2	atmos.: Honda2006 prompt: Sarcevic astro.: Astro.	SpiceLea	12646

Table 1.3: Overview of the datasets used for systematic uncertainties.

Generator	Type	Range [GeV]	Simulated γ	Weighted γ	Ice	Dataset	Syst. Eff.
CORS.	Hoerandel	$600 - 10^5$	Polygonato	GaisserH3a	SpiceLea	11527	DOM eff. -10%
CORS.	Hoerandel	$600 - 10^{11}$	Polygonato	GaisserH3a	SpiceLea	11526	DOM eff. +10%
CORS.	LE 5-comp.	$600 - 10^{11}$	2.6	GaisserH3a	SpiceLea	12388	Abs. +10% Scat. +10% Abs./Scat. -7.1%
CORS.	All datasets from Table 1.2			GaisserH4a	SpiceLea	Table 1.2	GaisserH4a
NuGen	ν_μ	$100 - 10^8$	2	Bartol (syst.)	SpiceLea	11029	Bartol flux
NuGen	ν_μ	$100 - 10^7$	2	Honda2006 + Bartol (syst.)	SpiceLea	11883	DOM eff. +10% DOM eff. -10% Abs. +10% Scat. +10% Abs./Scat. -7.1% Bartol flux
NuGen	ν_μ	$100 - 10^8$	2	Honda2006 + Bartol (syst.)	SpiceLea	12346	DOM eff. +10% DOM eff. -10% Abs./Scat. -7.1% Bartol flux

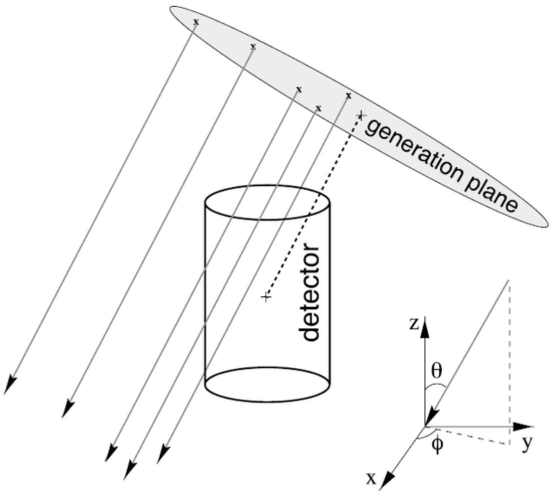

Figure 1.2: Illustration of how the particle injection works. The particle is first randomly positioned on a disk following a uniform distribution. The disk is then randomly rotated to simulate an isotropic flux.

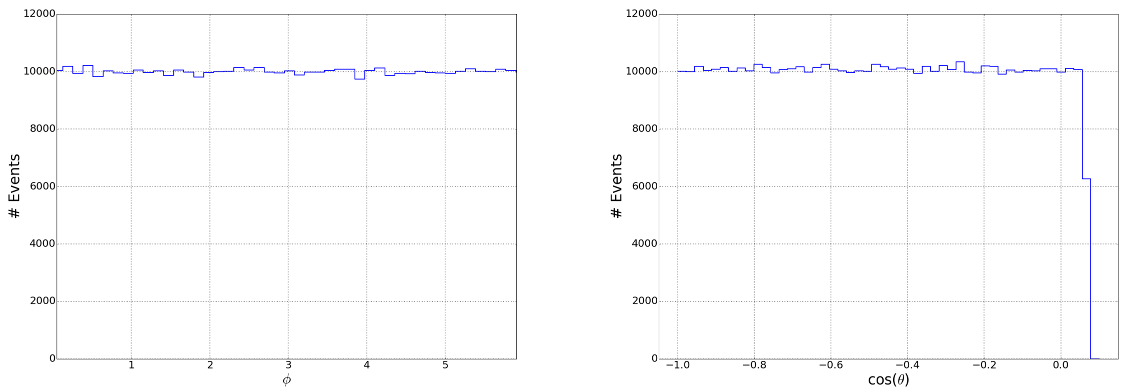

Figure 1.3: Illustration of uniform distributions of azimuth and cosine of the zenith for the particle injection in agreement with an isotropic flux (see Appendix **??**).

.

1.2.1 PROPOSAL

Using the cross sections of the important interaction, together with the properties of the traversing medium and the particles (mass, charge, spin, decay time, etc.) it is possible to simulate the energy losses, secondary production and the consequent interaction of these daughter particles. This is done in the software package (the Propagator with Optimal Precision and Optimized Speed for All Leptons), fully written in C++. It was based on the former program MMC (Muon Monte Carlo), which was written in Java. This year, a substantial improved version of PROPOSAL was finalized. An illustration of the workings of the code is given in Fig. 1.4 and an in depth documentation is given in Ref. [142].

PROPOSAL for SMPs

Since we assume the SMPs to behave leptonically, it was chosen to use PROPOSAL for the signal propagation as well. The mass and charge of the particle are set in the input parameters and the cross section dependence on these parameters can be seen in Section **??**. In general, there is a small dependence on the mass and a squared dependency on the charge (Eq. ???), except for bremsstrahlung that has a quadratic charge dependency. These effects only become prominent and important for highly relativistic particles, which as will be seen in Section ???, do

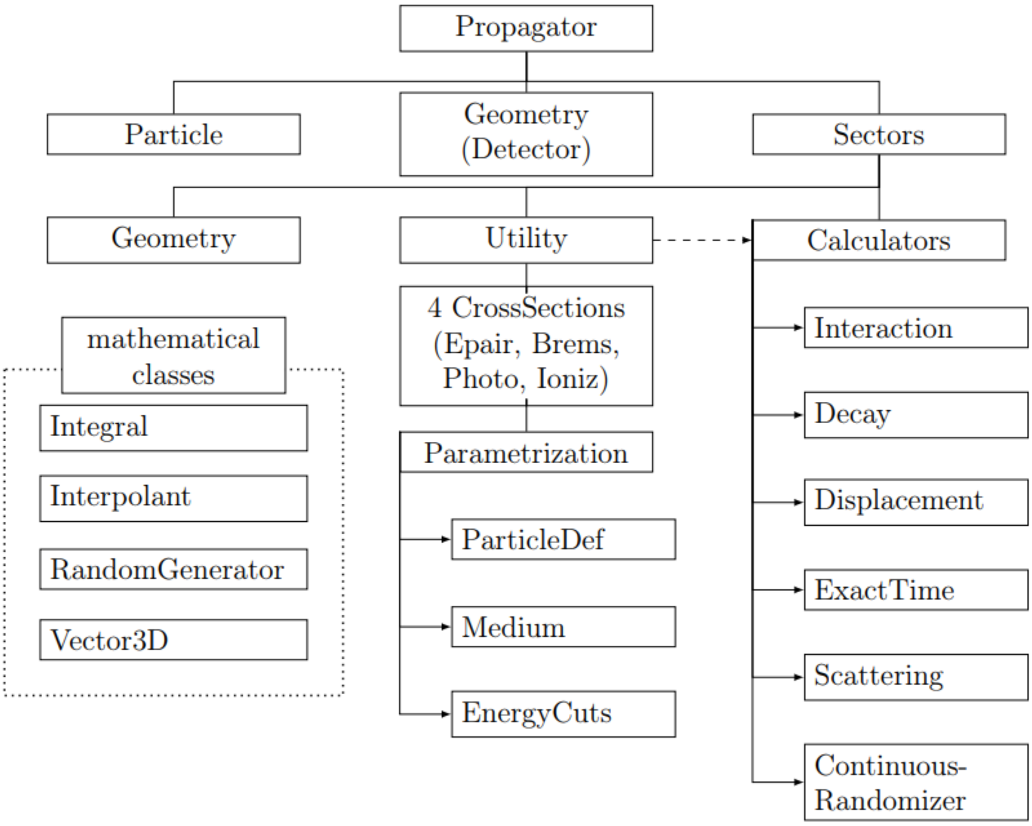

Figure 1.4: Overview of the class structure in PROPOSAL, from Ref. [142].

not have a dominating contribution to the total signal.

The PROPOSAL module keeps track of all the particles that are produced during propagation and the accompanying energy losses in a tree-like structure (called an *I3MCTree*). This collection of particles and their interactions are forwarded to a light production computation module.

1.2.2 Photoelectron generators

In Section **??** we already explained how the ice is simulated in the IceCube detector. The parameters $b_e(400)$ and ??? $a_{dust}(400)$ define the photon propagation through the ice and determine if they are absorbed or hit a DOM. To optimze computing time the DOMs were scaled (mostly with a factor of 5) to force more photon interactions. The number of photons emitted was then appropriately scaled down with the square of this scaling factor*. The DOM acceptance curves, as shown in Fig. **??**, together with the Frank-Tamm formula (Eq. **??**) allow to calculate the expected number of photons produced per unit length:

$$\frac{dN}{dx} = \int_{\lambda_1}^{\lambda_2} \frac{2\pi\alpha}{\lambda^2} \sin^2(\theta_c)\, d\lambda = 2\pi\alpha \sin^2(\theta_c) \left(\frac{1}{\lambda_1} - \frac{1}{\lambda_2}\right). \tag{1.3}$$

From this formula, we find that the expected rate of a Cherenkov emission profile is equal to ≈ 350 photons/cm. Together with the DOM acceptance, which has an overall average of around 7%, the expected *seen* number of photons per meter is equal to 2450 m^{-1}.

is a Photon Propagation Code, written in C++ and runs on graphic processing units (GPUs). This allows the code to run up to a hunderd times faster than in a CPU-only environment. employs both CUDA (NVIDIA GPU only) and OpenCL programming interface (both NVIDIA and AMD GPUs) together with multiple CPU environments. GPU environments allow the

*The surface of a sphere scales with the square of the radius.

tracking of thousands of photons simultaneously, vastly improving the computational speed. For more information, see Ref. [143].

Previous photon propagation code, such as [144], produced 6-dimensional photon tables (3 spatial, 2 directional and 1 temporal). This meant that at least one set of tables had to be produced per particle type and per velocity and interpolation methods had to be used, with the accompanying inaccuracies. These tables also required significant disk space and the method was therefore replaced with the GPU-codes. Direct photon simulation also allows for other non-trivial implementations such as the tilting of ice layers.

Another photon propagation code is , which uses GEANT4 to propagate particles. A hybrid version called *HybridCLsim* is sometimes where muons are propagated using / and their stochastic losses (which are showers) are simulated from tables whereas the "bare muons" (with their stochastics) are simulated using direct propagation. This avoids time loss for the rare but very computational high-energy cascade events.

photons in IC detector simulatie!

1.3 Detector simulation

polyplopia vuvuzela pmt domlauncher triggersim coincafterproc

1.4 Data processing

Getting the intricate details of nature just right is non-trivial. In many steps of the way, simulations use fits and estimations. Some simulation datasets are reasonable to compare to the data, depending on the phase space one is looking at, while other datasets need other specifications. For example, analyses dedicated to measuring the cosmic ray interactions need much more fine-tuning in their models for the atmosphere, composition, interaction models, etc. than an analysis dedicated to search for muon tracks that first propagated through the Earth and have atmospheric muons as a background.

It is for this reason, most analyses select a certain subset of the data they want to analyze to compare to the Monte Carlo simulations. For this analysis, it was chosen to look at 10% of the total data, called the . As indicated in Section [**subsec:datahandling**], the data is saved in 8-hour runs and the burn sample consists of every run ending with a '0'. The burn sample also allows to estimate the robustness of certain reconstructions and variables regarding differences in data and simulation.

More info see Section???

Hier ook een flowchart? Simulation documentation wiki mooi, samen met andere thesissen? Anna P?

1.5 Weighting

Maak ook een appendix waarbij je PDF van random numbers uitlegt!

Processing ergens: online L0, L1, L2, uw filters,...

2. Reconstruction and ???

2.1 IceHive

2.2 Line-Fit

Brenda Dingus thesis

2.3 SPE and MPE

2.4 Millipede

2.5 Boosted Decision Tree Classifiers

3. The SPACE Analysis

De uitleg van temperature modulations is goed in Sam zijn thesis `https://arxiv.org/pdf/physics/0312102v1.pdf`
`https://arxiv.org/pdf/1310.1284.pdf`

Ook ergens een tabel maken met info over je data runs. Duidelijk maken wat de livetime is bv en ook zeggen van wanneer to wanneer een bepaalde run liep (2011: mei 2011- mei 2012)

Klaus zijn paper? `https://arxiv.org/abs/1806.05696`

3.1 Motivation

3.2 General strategy

3.3 Event cleaning

3.4 Variables

3.5 BDT results

3.6 Pull validation

3.7 Systematic Uncertainties

3.8 Results

4. Summary and Discussion

Appendices

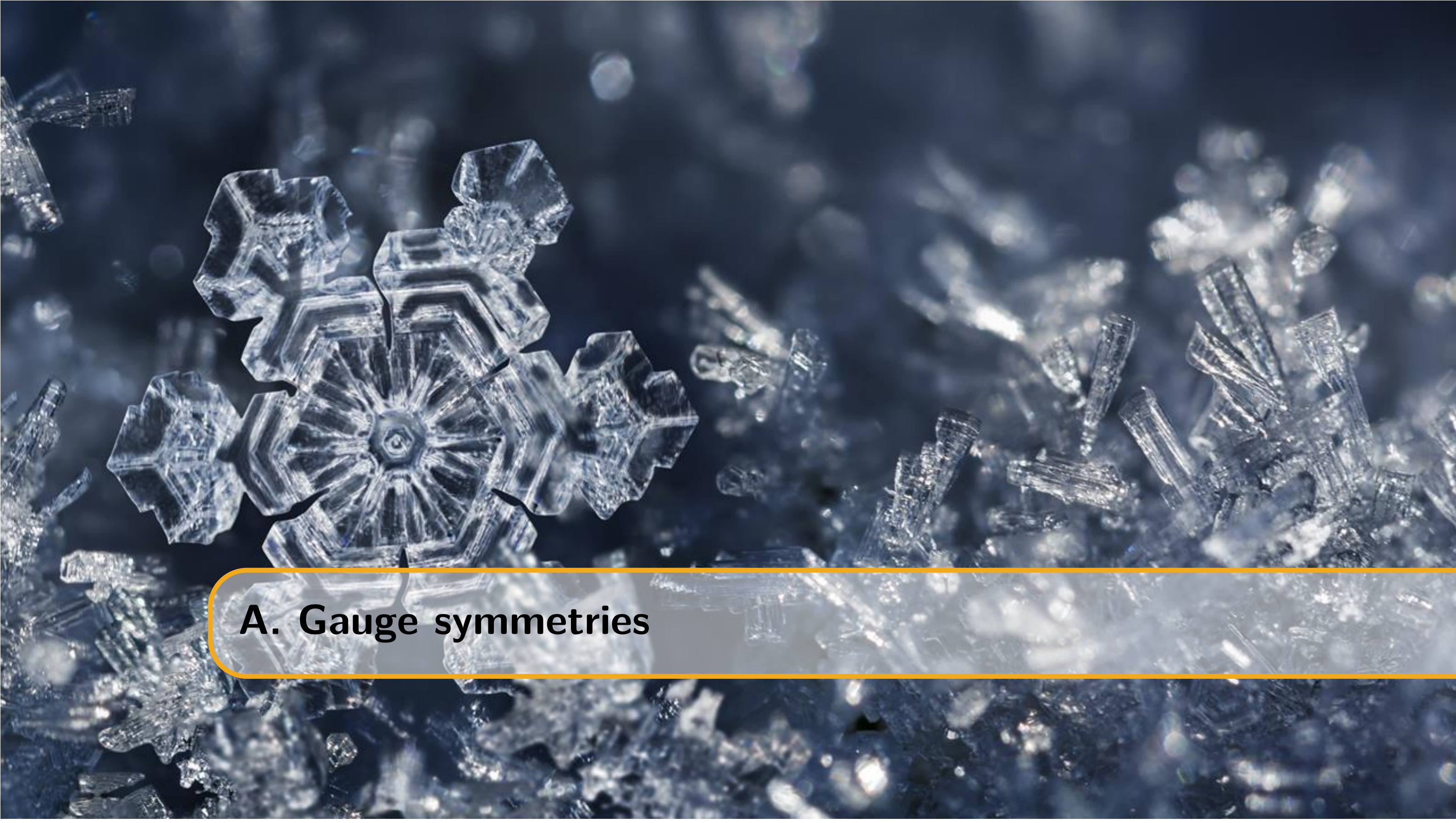

A. Gauge symmetries

NOG NIET GEDAAN

The difference between global and local symmetries are not straightforward for everybody. In this appendix I try to give a better view of the matter.

Imagine that at each point in space and time there is a circle attached to it. If one shifts all circles of all points with a fixed angle the underlying physics hasn't changed. If we look at the whole in a different angle, nothing seems to be changed as everything holds the same relative orientation. This is a global symmetry. For local symmeries we instead shift each circle through a different angle, but an angle that changes smoothly from point to point and in a way that we can say how that angle is varying between different nearby regions. Then it will turn out that we can describe that rotation angle by means of a so-called gauge field, which just lets us transport the charged scalar field from one point in space time to another, taking account of how the rotation angle of the circle is changing. A gauge is a kind of coordinate system that is varying depending on the location with respect to some underlying space. In physics we are almost always concerned with space-time as the underlying space, and we are typically interested in theories that are invariant with respect to the choice of gauge or coordinate system.

Dan wat uitleg vanuit je QFT boek en de dingen hieronder: Je wilt je derivative anders doen werken in je theory onder een transformatie, maar daarvoor heb je een veld nodig. M.a.w.: dankzij een veld heb je lokale ijktransformatie mogelijk!

B. Planck's law

bron: http://hyperphysics.phy-astr.gsu.edu/hbase/quantum/rayj.html

B.1 Electromagnetic waves in a cubical cavity

Suppose we have EM waves in a cavity at equilibrium with its surroundings. These waves must satisfy the wave equation in three dimensions:

$$\frac{\partial^2\Psi}{\partial x^2} + \frac{\partial^2\Psi}{\partial y^2} + \frac{\partial^2\Psi}{\partial z^2} = \frac{1}{c^2}\frac{\partial^2\Psi}{\partial t^2}. \tag{B.1}$$

The solution must give zero amplitude at the walls. A non-zero value would mean energy is dissipated through the walls which is in contradiction to our equilibrium assumption. A general solution takes the form of

$$\Psi(x,y,z,t) = \Psi_0 \sin k_1 x \sin k_2 y \sin k_3 z \sin k_4 t, \tag{B.2}$$

which, after requiring $k_n L = n\pi$ with $n = 0, 1, 2...$ and $k_4 \frac{\lambda}{2c} = \pi$, leads to

$$\Psi(x,y,z,t) = \Psi_0 \sin\left(\frac{n_1 \pi x}{L}\right) \sin\left(\frac{n_2 \pi y}{L}\right) \sin\left(\frac{n_3 \pi z}{L}\right) \sin\left(\frac{2\pi c t}{\lambda}\right). \tag{B.3}$$

From the wave equation it is easy to find that

$$n^2 = n_1^2 + n_2^2 + n_3^2 = \frac{4L^2}{\lambda^2}, \tag{B.4}$$

which span up a sphere in "n-space" with a volume of $\frac{1}{8}\frac{4}{3}\pi n^{3/2}$, where the first term originates from the positive nature of $n_{1,2,3}$. Because there are two possible polarizations of the waves one has to multiply with an additional factor 2. The number of modes per unit wavelength is equal to

$$\frac{dN}{d\lambda} \times \frac{1}{L^3} = \frac{d}{d\lambda}\left[\frac{8\pi L^3}{3\lambda^3}\right] \times \frac{1}{L^3} = -\left[\frac{8\pi}{\lambda^4}\right]. \tag{B.5}$$

B.1.1 Classical approach

Following the principle of equipartition of energy, each standing wave mode will have an average enkergy kT with k the Boltzmann constant and T the temperature in Kelvin. The energy density is then:

$$\frac{du}{d\lambda} = -kT\frac{8\pi}{\lambda^4}. \tag{B.6}$$

In function of frequency $\nu = \frac{c}{\lambda}$:

$$\frac{du}{d\nu} = -\frac{c}{\lambda^2}\frac{du}{d\lambda} = \frac{8\pi kT\nu^2}{c^3}, \tag{B.7}$$

also known as the Rayleigh-Jeans law*. Problem: divergence

B.1.2 Quantum approach

The energy levels from a quantized harmonic oscillator are equal to

$$E_r = h\nu\left(r + \frac{1}{2}\right) = \frac{hc}{\lambda}\left(r + \frac{1}{2}\right) \quad \text{with} r = 0, 1, 2, ... \tag{B.8}$$

Implementing eq. B.4

$$E = \left(r + \frac{1}{2}\right)\frac{hc}{2L}\sqrt{n_1^2 + n_2^2 + n_3^2} \tag{B.9}$$

According to statistical physics the average energy is now not equal to kT but follows a probability distribution

$$p(\nu, r) = \frac{e^{\frac{-rh\nu}{kT}}}{\sum_{r=0}^{\infty} e^{\frac{-rh\nu}{kT}}}, \tag{B.10}$$

where we reference to the ground state of the oscillator: $E'_r = E_r - E_0$.

The average energy is now:

$$\begin{aligned}\langle E(\nu)\rangle &= \sum_{r=0}^{\infty} E(\nu, r)\cdot p(\nu, r) = \frac{\sum_{r=0}^{\infty} rh\nu\ e^{\frac{-rh\nu}{kT}}}{\sum_{r=0}^{\infty} e^{\frac{-rh\nu}{kT}}} \\ &= \frac{h\nu}{e^{h\nu/kT} - 1}\end{aligned} \tag{B.11}$$

Substituting this for kT in eq. B.7 we find Planck's equation:

$$\frac{du}{d\nu} = \frac{8\pi h\nu^3}{c^3}\frac{h\nu}{e^{h\nu/kT} - 1} \tag{B.12}$$

*This is often quoted per unit of staradian, which results in $\frac{2kT\nu^2}{c^3}$

C. Statistics

A word that is often mentioned in this work is “statistics”. It refers to the statistical error of a counting experiment, i.e. the Poissonian error. The Poisson distribution is a discrete probability of a certain number of $n$events occurring in a fixed time interval. The Poisson probability function is given by

$$P(n) = \frac{\lambda^n e^{-\lambda}}{n!}, \tag{C.1}$$

where λ is the expected number of events and also equal to the variance. An experiment that counted N events therefore has a statistical error of

$$\sigma = \sqrt{N} \tag{C.2}$$

In other words: higher statistics denotes a lower statistical error.

D. Distributions

D.1 Spherical random numbers

Most random number generators provide uniform distributions from between the range [01,]. Assume we want to make a uniform distribution along a sphere with angles ϕ and θ and radius r, in spherical coordinates. Random numbers between $[0, \pi]$, $[0, 2\pi]$ and $[0, R]$ (the ranges of the coordinates) would not give a uniform distribution as illustrated in Fig. D.1 (left).
The differential surface area, dA, is equal to $dA(d\phi, d\theta) = r^2 \sin(\phi) d\phi d\theta$. If we want the distribution $f(v)$ to be constant for a uniform distribution, then $f(v) = \frac{1}{4\pi}$ since $\int\int_S f(v) dA = 1$ and $\int\int_S dA = 4\pi$. We want the distribution in function of the angles, so

$$f(v) dA = \frac{1}{4\pi} dA = f(\phi, \theta) d\phi d\theta. \tag{D.1}$$

Since we know the expression for dA, we find that

$$f(\phi, \theta) = \frac{1}{4\pi} \sin(\phi), \tag{D.2}$$

and separating the angles:

$$f(\theta) = \int_0^{\pi} f(\phi, \theta) d\phi = \frac{1}{2\pi}, \tag{D.3}$$

$$f(\phi) = \int_0^{2\pi} f(\phi, \theta) d\theta = \frac{\sin(\phi)}{2}, \tag{D.4}$$

where it is clear that $f(\pi)$ scales with $\sin(\phi)$; there are more points needed at the equator (this makes sense, as the total surface at the equator is much larger!).

The question is now how one can get a sample to follow the distribution of $f(\phi)$. For this, we use the *inverse transform sampling* method where one makes use of the cumulative distribution function, $F(\phi)$, which increases monotonically

$$F(\phi) = \int_0^{\phi} f(\phi') d\phi' = \frac{1}{2} (1 - \cos(\phi)). \tag{D.5}$$

The method shows that if u is a random variable drawn from a uniform distribution, we have to find the inverse function of F,

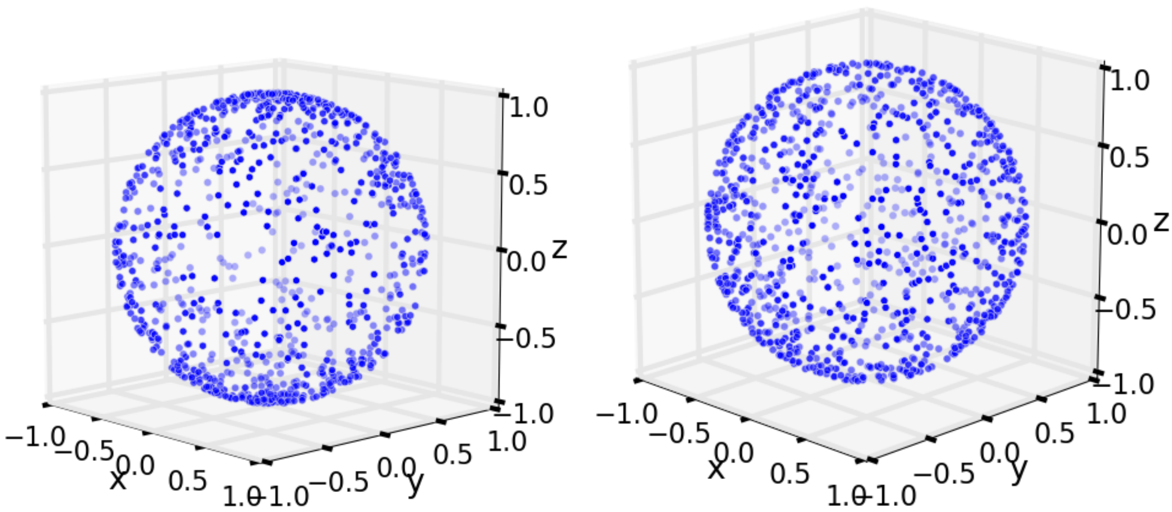

Figure D.1: Blub

$$F(F^{-1}(u)) = u \tag{D.6}$$

$$\frac{1}{2}\left(1 - \cos(F^{-1}(u))\right) = u \tag{D.7}$$

$$F^{-1}(u) = \arccos(1 - 2u). \tag{D.8}$$

In other words: if u is a random variable drawn from a uniform distribution, then $\phi = \arccos(1-2u)$ follows a distribution necessary for a uniform spherical distribution. Similarly, $\theta = \frac{1}{2\pi}u$.

D.2 Power law distributions

Analogous to what was written in the previous section, one can produce a power law distribution from random numbers using the inverse transform sampling method:

$$\begin{aligned}
f(E) &= A \cdot E^{-\gamma} \quad \text{(powerlaw)} \\
F(E) &= \int_{E_{min}}^{E} A \cdot E^{-\gamma} dE = u \quad \text{(inverse sampling, u random number [} \\
&= A \left[\frac{E^{-\gamma+1}}{-\gamma+1} \right]_{E_{min}}^{E} \\
&= \frac{A}{-\gamma+1} \left(E^{-\gamma+1} - E_{min}^{-\gamma+1} \right) \\
F\left(F^{-1}(u)\right) &= u \\
&\Rightarrow \\
u &= \frac{A}{-\gamma+1} \left(\left(F^{-1}(u)\right)^{-\gamma+1} - E_{min}^{-\gamma+1} \right) \\
F^{-1}(u) &= \left(\left(\frac{-\gamma+1}{A} \cdot u \right) + E_{min}^{-\gamma+1} \right)^{1/(-\gamma+1)} \\
&\text{and because} \\
F(E_{max}) = 1 \Rightarrow A &= \frac{-\gamma+1}{E_{max}^{-\gamma+1} - E_{min}^{-\gamma+1}} \\
&\Rightarrow \\
F^{-1}(u) &= \left((1-u) \cdot E_{min}^{-\gamma+1} + u \cdot E_{max}^{-\gamma+1} \right)^{1/(-\gamma+1)}
\end{aligned}$$

E will follow from the distribution $f(E)$ as

$$E = \left((1-u) \cdot E_{min}^{-\gamma+1} + u \cdot E_{max}^{-\gamma+1} \right)^{1/(-\gamma+1)} \tag{D.9}$$

For γ = -1, we will make a uniform distribution in log space. This is shown in Fig. D.2.

$$\begin{aligned}
E &= E_{min} \cdot 10^{u \cdot \log \frac{E_{max}}{E_{min}}} \\
&= 10^{u[\log E_{min}, \log E_{max}]}
\end{aligned} \tag{D.10}$$

D.3 Angular distributions

As seen in Section D.1, the differential space angle $d\Omega$ is equal to

$$d\Omega = \sin\theta d\theta d\phi. \tag{D.11}$$

If one shows the distribution of ϕ and/or θ, then this is the same as showing partial integrations per bin. We find that

$$\Omega \propto \cos\theta\phi, \tag{D.12}$$

or in other words: the space angle is proportional to the azimuth and the cosine of the zenith. An example is shown in Fig. **??**.

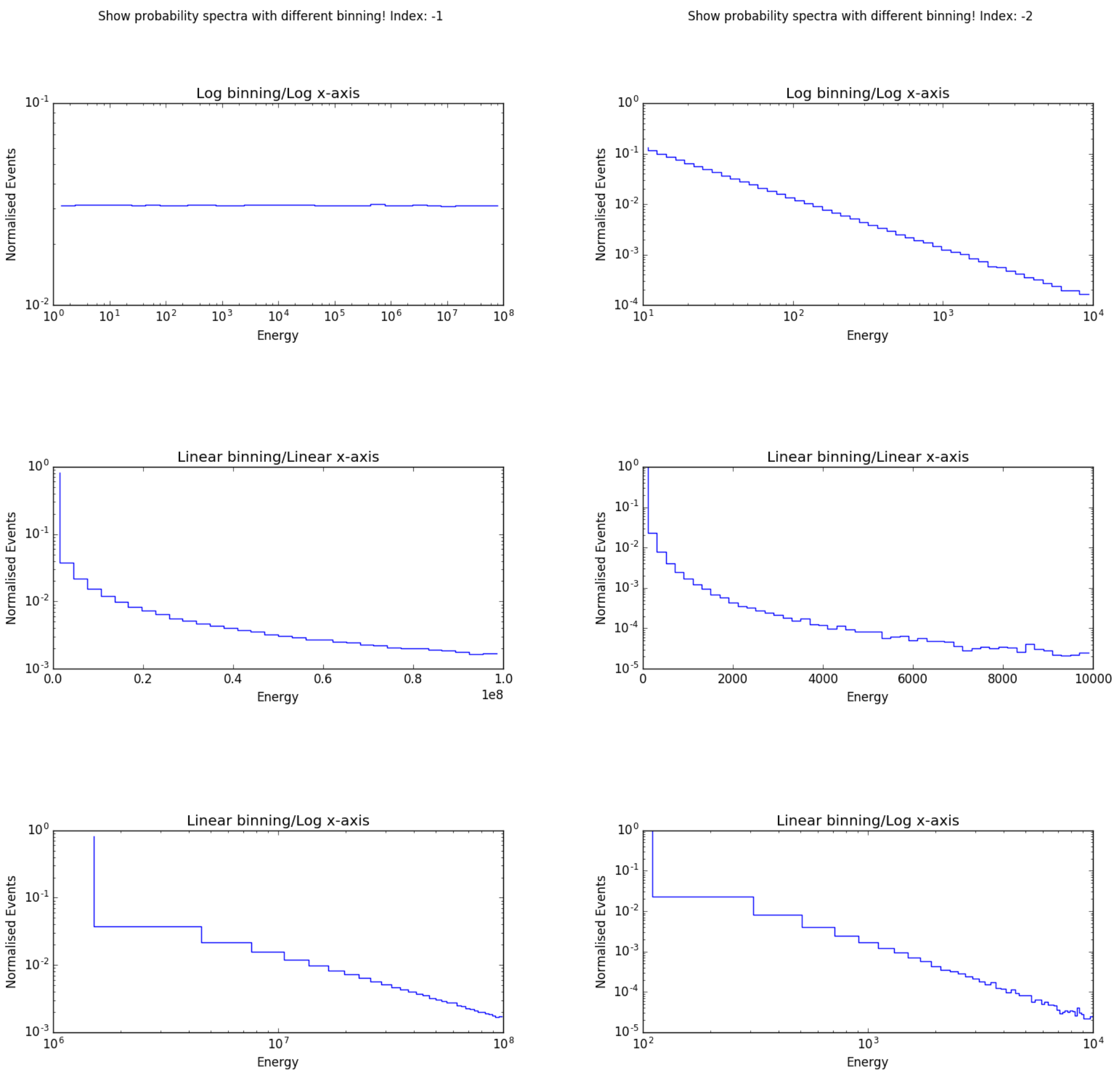

Figure D.2: Blub

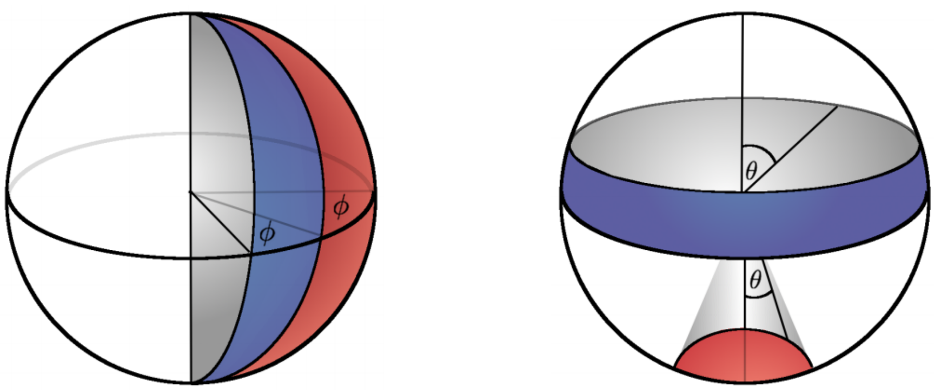

Figure D.3: Illustration of angle distributions in spherical coordinates. The blue and red surfaces are equal in size. The left figure clearly shows the surface to be proportional to the azumith. The right figure shows how there is a non-trivial dependence on the zenith angle for equal partitions on the surface of a sphere.

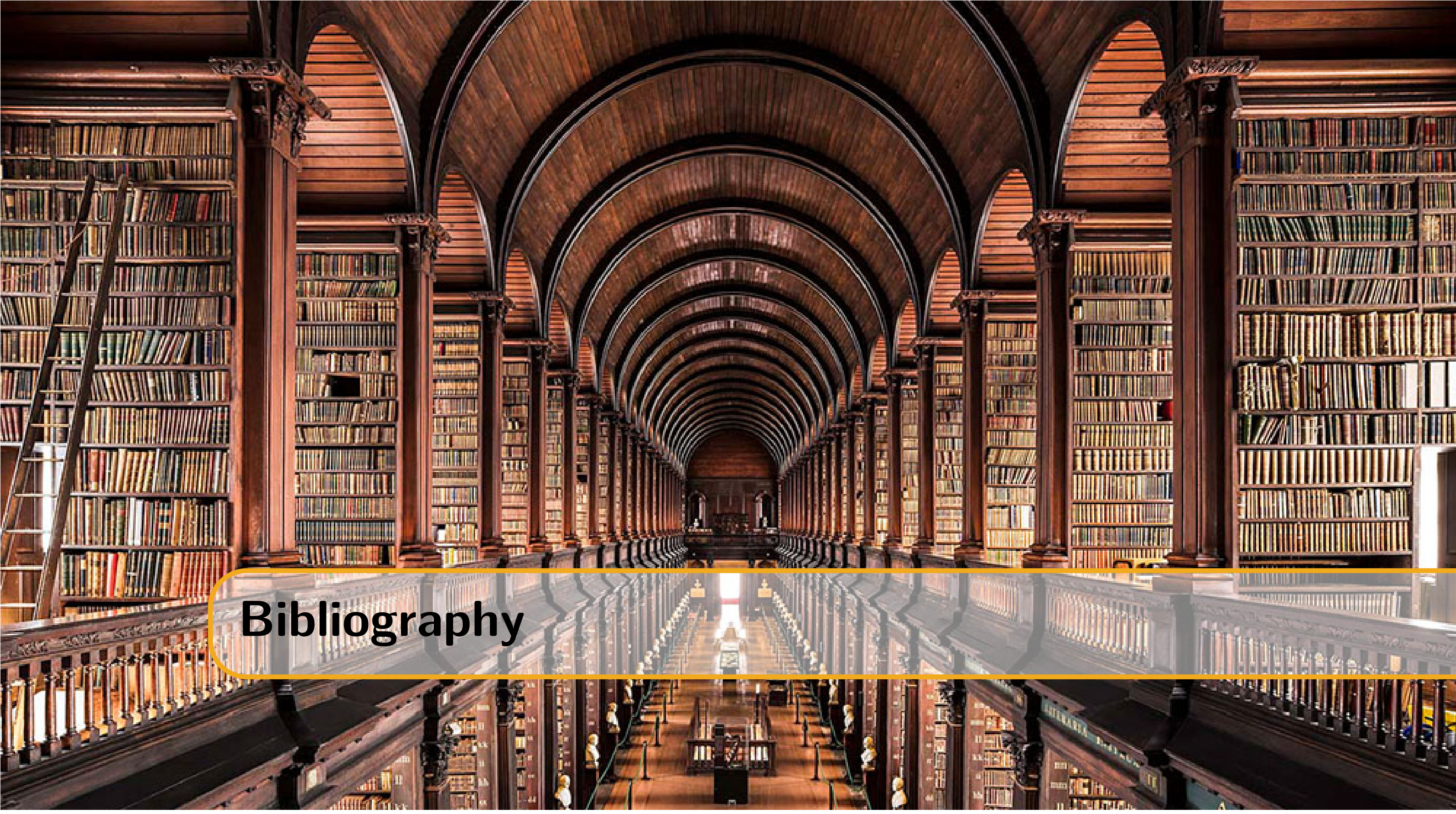

Bibliography

[1] B. Povh et al. *Particles and nuclei: An Introduction to the physical concepts*. 1995. DOI: 10.1007/3-540-36684-9.

[2] Michael E. Peskin and Daniel V. Schroeder. *An Introduction to quantum field theory*. Reading, USA: Addison-Wesley, 1995. ISBN: 9780201503975, 0201503972. URL: http://www.slac.stanford.edu/~mpeskin/QFT.html.

[3] M. Tanabashi et al. "Review of Particle Physics". In: *Phys. Rev. D* 98 (2018), page 030001.

[4] Alessandro Bettini. *Introduction to elementary particle physics*. 2008. ISBN: 9780521880213. URL: http://www.cambridge.org/catalogue/catalogue.asp?isbn=9780521880213.

[5] CERN. URL: https://home.cern/about/physics/standard-model.

[6] Arthur B. McDonald. "Nobel Lecture: The Sudbury Neutrino Observatory: Observation of flavor change for solar neutrinos". In: *Rev. Mod. Phys.* 88 (3 July 2016), page 030502. DOI: 10.1103/RevModPhys.88.030502. URL: https://link.aps.org/doi/10.1103/RevModPhys.88.030502.

[7] CMS. URL: http://cms.web.cern.ch/news/jets-cms-and-determination-their-energy-scale.

[8] A. Kircher. *Athanasii Kircherii... Magnes, sive De arte magnetica opus tripartitum...* sumptibus H. Scheus, 1641. URL: https://books.google.be/books?id=1aZ3FcTAYdUC.

[9] G. Farmelo. *The Strangest Man: The Hidden Life of Paul Dirac, Mystic of the Atom*. Basic Books, 2009. ISBN: 9780465019922. URL: https://books.google.be/books?id=qsodmIGD0fMC.

[10] F. Mandl and G. Shaw. *Quantum Field Theory*. Wiley, 2013. ISBN: 9781118716656. URL: https://books.google.be/books?id=jTBzQfctvHAC.

[11] Flip Tanedo. URL: https://www.quantumdiaries.org/2012/02/14/why-do-we-expect-a-higgs-boson-part-ii-unitarization-of-vector-boson-scattering/.

[12] S. L. Glashow, J. Iliopoulos, and L. Maiani. "Weak Interactions with Lepton-Hadron Symmetry". In: *Phys. Rev.* D2 (1970), pages 1285–1292. DOI: 10.1103/PhysRevD.2.1285.

[13] J. H. Christenson et al. "Evidence for the 2π Decay of the K20 Meson". In: *Physical Review Letters* 13 (July 1964), pages 138–140. DOI: 10.1103/PhysRevLett.13.138.

[14] Ziro Maki, Masami Nakagawa, and Shoichi Sakata. "Remarks on the Unified Model of Elementary Particles". In: *Progress of Theoretical Physics* 28.5 (1962), pages 870–880. DOI: 10.1143/PTP.28.870. eprint: /oup/backfile/content_public/journal/ptp/28/5/10.1143/ptp.28.870/2/28-5-870.pdf. URL: http://dx.doi.org/10.1143/PTP.28.870.

[15] Unknown. *Young interference*. https://www.shmoop.com/optics/young-double-slit.html. [Online; accessed August 2018]. 2018.

[16] Antoine Weis and Robert Wynands. "Three Demonstration Experiments on the Wave and Particle Nature of Light". In: 1 (June 2003).

[17] C. Davisson and L. H. Germer. "Diffraction of Electrons by a Crystal of Nickel". In: *Phys. Rev.* 30 (1927), pages 705–740. DOI: 10.1103/PhysRev.30.705.

[18] G P. Thomson and Reid AA. "Diffraction of Cathode Rays by a Thin Film". In: 119 (Jan. 1927), pages 890–890.

[19] Claus Jönsson. "Elektroneninterferenzen an mehreren künstlich hergestellten Feinspalten". In: *Zeitschrift für Physik* 161.4 (Aug. 1961), pages 454–474. ISSN: 0044-3328. DOI: 10.1007/BF01342460. URL: https://doi.org/10.1007/BF01342460.

[20] P G Merli, G F Missiroli, and G Pozzi. "Electron interferometry with the Elmiskop 101 electron microscope". In: *Journal of Physics E: Scientific Instruments* 7.9 (1974), page 729. URL: http://stacks.iop.org/0022-3735/7/i=9/a=016.

[21] C. D. Anderson. "The Positive Electron". In: *Phys. Rev.* 43 (1933), pages 491–494. DOI: 10.1103/PhysRev.43.491.

[22] Paul A. M. Dirac. "The quantum theory of the electron". In: *Proc. Roy. Soc. Lond.* A117 (1928), pages 610–624. DOI: 10.1098/rspa.1928.0023.

[23] C. M. G. Lattes et al. "PROCESSES INVOLVING CHARGED MESONS". In: *Nature* 159 (1947). [,42(1947)], pages 694–697. DOI: 10.1038/159694a0.

[24] S. H. Neddermeyer and C. D. Anderson. "Note on the Nature of Cosmic Ray Particles". In: *Phys. Rev.* 51 (1937), pages 884–886. DOI: 10.1103/PhysRev.51.884.

[25] S. W. Herb et al. "Observation of a Dimuon Resonance at 9.5-GeV in 400-GeV Proton-Nucleus Collisions". In: *Phys. Rev. Lett.* 39 (1977), pages 252–255. DOI: 10.1103/PhysRevLett.39.252.

[26] F. Abe et al. "Observation of top quark production in $\bar{p}p$ collisions". In: *Phys. Rev. Lett.* 74 (1995), pages 2626–2631. DOI: 10.1103/PhysRevLett.74.2626. arXiv: hep-ex/9503002 [hep-ex].

[27] D. P. Barber et al. "Discovery of Three Jet Events and a Test of Quantum Chromodynamics at PETRA Energies". In: *Phys. Rev. Lett.* 43 (1979), page 830. DOI: 10.1103/PhysRevLett.43.830.

[28] S. Schael et al. "Precision electroweak measurements on the Z resonance". In: *Phys. Rept.* 427 (2006), pages 257–454. DOI: 10.1016/j.physrep.2005.12.006. arXiv: hep-ex/0509008 [hep-ex].

[29] Sabine Riemann. "Precision electroweak physics at high energies". In: *Rept. Prog. Phys.* 73 (2010), page 126201. DOI: 10.1088/0034-4885/73/12/126201.

[30] Kenji Abe et al. "A High precision measurement of the left-right Z boson cross-section asymmetry". In: *Phys. Rev. Lett.* 84 (2000), pages 5945–5949. DOI: 10.1103/PhysRevLett.84.5945. arXiv: hep-ex/0004026 [hep-ex].

[31] Koya Abe et al. "First direct measurement of the parity violating coupling of the Z0 to the s quark". In: *Phys. Rev. Lett.* 85 (2000), pages 5059–5063. DOI: 10.1103/PhysRevLett.85.5059. arXiv: hep-ex/0006019 [hep-ex].

[32] Koya Abe et al. "An Improved direct measurement of leptonic coupling asymmetries with polarized Z bosons". In: *Phys. Rev. Lett.* 86 (2001), pages 1162–1166. DOI: 10.1103/PhysRevLett.86.1162. arXiv: hep-ex/0010015 [hep-ex].

[33] K. Abe et al. “First measurement of the left-right charge asymmetry in hadronic Z boson decays and a new determination of sin**2 theta(W)(eff)”. In: *Phys. Rev. Lett.* 78 (1997), pages 17–21. DOI: 10.1103/PhysRevLett.78.17. arXiv: hep-ex/9609019 [hep-ex].

[34] Timo Antero Aaltonen et al. “Combination of CDF and D0 W-Boson Mass Measurements”. In: *Phys. Rev.* D88.5 (2013), page 052018. DOI: 10.1103/PhysRevD.88.052018. arXiv: 1307.7627 [hep-ex].

[35] “Combination of CDF and D0 Results on the Width of the W boson”. In: (2010). arXiv: 1003.2826 [hep-ex].

[36] Morad Aaboud et al. “Measurement of the W-boson mass in pp collisions at $\sqrt{s} = 7$ TeV with the ATLAS detector”. In: *Eur. Phys. J.* C78.2 (2018), page 110. DOI: 10.1140/epjc/s10052-017-5475-4. arXiv: 1701.07240 [hep-ex].

[37] ATLAS. URL: cds.cern.ch/record/2285809/files/ATLAS-CONF-2017-071.pdf.

[38] CMS. URL: cds.cern.ch/record/2235162/files/TOP-15-012-pas.pdf.

[39] CMS. URL: cds.cern.ch/record/2284594/files/TOP-17-007-pas.pdf.

[40] PDG. URL: http://pdg.lbl.gov/2018/reviews/rpp2018-rev-standard-model.pdf.

[41] P. A. R. Ade et al. “Planck 2015 results. XIII. Cosmological parameters”. In: *Astron. Astrophys.* 594 (2016), A13. DOI: 10.1051/0004-6361/201525830. arXiv: 1502.01589 [astro-ph.CO].

[42] Edvige Corbelli and Paolo Salucci. “The Extended Rotation Curve and the Dark Matter Halo of M33”. In: *Mon. Not. Roy. Astron. Soc.* 311 (2000), pages 441–447. DOI: 10.1046/j.1365-8711.2000.03075.x. arXiv: astro-ph/9909252 [astro-ph].

[43] S. M. Faber and R. E. Jackson. “Velocity dispersions and mass to light ratios for elliptical galaxies”. In: *Astrophys. J.* 204 (1976), page 668. DOI: 10.1086/154215.

[44] Steven W. Allen, August E. Evrard, and Adam B. Mantz. “Cosmological Parameters from Observations of Galaxy Clusters”. In: *Ann. Rev. Astron. Astrophys.* 49 (2011), pages 409–470. DOI: 10.1146/annurev-astro-081710-102514. arXiv: 1103.4829 [astro-ph.CO].

[45] Priyamvada Natarajan et al. “Mapping substructure in the HST Frontier Fields cluster lenses and in cosmological simulations”. In: *Mon. Not. Roy. Astron. Soc.* 468.2 (2017), pages 1962–1980. DOI: 10.1093/mnras/stw3385. arXiv: 1702.04348 [astro-ph.GA].

[46] Edwin Hubble. “A relation between distance and radial velocity among extra-galactic nebulae”. In: *Proc. Nat. Acad. Sci.* 15 (1929), pages 168–173. DOI: 10.1073/pnas.15.3.168.

[47] John F. Donoghue. “The effective field theory treatment of quantum gravity”. In: *AIP Conf. Proc.* 1483 (2012), pages 73–94. DOI: 10.1063/1.4756964. arXiv: 1209.3511 [gr-qc].

[48] J. L. Holzbauer. “The Muon g-2 Experiment Overview and Status”. In: *PoS* NuFact2017 (2018), page 116. DOI: 10.22323/1.295.0116. arXiv: 1712.05980 [hep-ex].

[49] Alexandre Deur, Stanley J. Brodsky, and Guy F. de Teramond. “The QCD Running Coupling”. In: *Prog. Part. Nucl. Phys.* 90 (2016), pages 1–74. DOI: 10.1016/j.ppnp.2016.04.003. arXiv: 1604.08082 [hep-ph].

[50] nobel2004. URL: https://www.nobelprize.org/prizes/physics/2004/popular-information/.

[51] Xiao-Gang He, Girish C. Joshi, and B. H. McKellar. “The Quantization of the Electric Charge in Gauge Theories”. In: *Europhys. Lett.* 10 (1989), page 709. DOI: 10.1209/0295-5075/10/8/002.

[52] Hong-Wei Yu. “SU(8) GUT MODELS WITH STABLE PROTON, N ANTI-N OSCILLATIONS, FRACTIONAL CHARGES AND LOW MASS MONOPOLES”. In: *Phys. Lett.* 142B (1984), pages 42–46. DOI: 10.1016/0370-2693(84)91132-8.

[53] Stephen M. Barr, D. B. Reiss, and A. Zee. "Fractional Charges, Monopoles and Peculiar Photons". In: *Phys. Rev. Lett.* 50 (1983), page 317. DOI: 10.1103/PhysRevLett.50.317.

[54] P. H. Frampton and T. W. Kephart. "Fractionally Charged Particles as Evidence for Supersymmetry". In: *Phys. Rev. Lett.* 49 (1982), page 1310. DOI: 10.1103/PhysRevLett.49.1310.

[55] Katsuji Yamamoto. "Fractionally Charged Leptons in the SO(14) GUT". In: *Phys. Lett.* 120B (1983), pages 157–160. DOI: 10.1016/0370-2693(83)90643-3.

[56] Fang-xiao Dong et al. "Fractional Charges, Monopoles and Peculiar Photons in SO(18) GUT Models". In: *Phys. Lett.* 129B (1983), pages 405–410. DOI: 10.1016/0370-2693(83)90129-6.

[57] Xiang-Dong Jiang and Xian-Jian Zhou. "SO(10) X SO(8) MODEL WITH FRACTIONAL CHARGES, MONOPOLES AND PECULIAR PHOTONS. (IN CHINESE)". In: *HEPNP* 9 (1985), pages 421–429.

[58] Borut Bajc et al. "Threshold corrections to dimension-six proton decay operators in non-minimal SUSY SU (5) GUTs". In: *Nucl. Phys.* B910 (2016), pages 1–22. DOI: 10.1016/j.nuclphysb.2016.06.017. arXiv: 1603.03568 [hep-ph].

[59] H. Nishino et al. "Search for Proton Decay via p —> e+ pi0 and p —> mu+ pi0 in a Large Water Cherenkov Detector". In: *Phys. Rev. Lett.* 102 (2009), page 141801. DOI: 10.1103/PhysRevLett.102.141801. arXiv: 0903.0676 [hep-ex].

[60] Xiao-Gang Wen and Edward Witten. "Electric and Magnetic Charges in Superstring Models". In: *Nucl. Phys.* B261 (1985), pages 651–677. DOI: 10.1016/0550-3213(85)90592-9.

[61] Ignatios Antoniadis and K. Benakli. "Fractionally charged particles and supersymmetry breaking in 4-D strings". In: *Phys. Lett.* B295 (1992). [Erratum: Phys. Lett.B407,449(1997)], pages 219–224. DOI: 10.1016/S0370-2693(97)00755-7,10.1016/0370-2693(92)91557-P. arXiv: hep-th/9209020 [hep-th].

[62] Gregory G. Athanasiu et al. "Remarks on Wilson Lines, Modular Invariance and Possible String Relics in Calabi-yau Compactifications". In: *Phys. Lett.* B214 (1988), pages 55–62. DOI: 10.1016/0370-2693(88)90451-0.

[63] Bob Holdom. "Two U(1)'s and Epsilon Charge Shifts". In: *Phys. Lett.* 166B (1986), pages 196–198. DOI: 10.1016/0370-2693(86)91377-8.

[64] Eder Izaguirre and Itay Yavin. "New window to millicharged particles at the LHC". In: *Phys. Rev.* D92.3 (2015), page 035014. DOI: 10.1103/PhysRevD.92.035014. arXiv: 1506.04760 [hep-ph].

[65] David E. Brahm and Lawrence J. Hall. "U(1)-prime DARK MATTER". In: *Phys. Rev.* D41 (1990), page 1067. DOI: 10.1103/PhysRevD.41.1067.

[66] C. Boehm and Pierre Fayet. "Scalar dark matter candidates". In: *Nucl. Phys.* B683 (2004), pages 219–263. DOI: 10.1016/j.nuclphysb.2004.01.015. arXiv: hep-ph/0305261 [hep-ph].

[67] Maxim Pospelov, Adam Ritz, and Mikhail B. Voloshin. "Secluded WIMP Dark Matter". In: *Phys. Lett.* B662 (2008), pages 53–61. DOI: 10.1016/j.physletb.2008.02.052. arXiv: 0711.4866 [hep-ph].

[68] James D. Bjorken et al. "New Fixed-Target Experiments to Search for Dark Gauge Forces". In: *Phys. Rev.* D80 (2009), page 075018. DOI: 10.1103/PhysRevD.80.075018. arXiv: 0906.0580 [hep-ph].

[69] Gabriel Magill et al. "Millicharged particles in neutrino experiments". In: (2018). arXiv: 1806.03310 [hep-ph].

[70] R. Acciarri et al. "Long-Baseline Neutrino Facility (LBNF) and Deep Underground Neutrino Experiment (DUNE)". In: (2015). arXiv: 1512.06148 [physics.ins-det].

[71] M. Anelli et al. "A facility to Search for Hidden Particles (SHiP) at the CERN SPS". In: (2015). arXiv: 1504.04956 [physics.ins-det].

[72] Marco Battaglieri et al. "US Cosmic Visions: New Ideas in Dark Matter 2017: Community Report". In: (2017). arXiv: 1707.04591 [hep-ph].

[73] L. Lyons. "Quark Search Experiments at Accelerators and in Cosmic Rays". In: *Phys. Rept.* 129 (1985), page 225. DOI: 10.1016/0370-1573(85)90011-0.

[74] J. J. Aubert et al. "A Search for Free Quarks in Deep Inelastic Muon Scattering". In: *Phys. Lett.* 133B (1983), page 461. DOI: 10.1016/0370-2693(83)90828-6.

[75] A. E. Bondar et al. "SEARCH FOR LIGHT PARTICLES WITH CHARGE 2/3 IN e+ e- ANNIHILATION". In: *JETP Lett.* 40 (1984). [Pisma Zh. Eksp. Teor. Fiz.40,440(1984)], pages 1265–1268.

[76] H. Aihara et al. "Search for $q = 2/3e$ and $q = 1/3e$ particles produced in e^+e^- annihilations". In: *Phys. Rev. Lett.* 52 (1984), page 2332. DOI: 10.1103/PhysRevLett.52.2332.

[77] G. Abbiendi et al. "Search for stable and longlived massive charged particles in e+ e- collisions at s**(1/2) = 130-GeV to 209-GeV". In: *Phys. Lett.* B572 (2003), pages 8–20. DOI: 10.1016/S0370-2693(03)00639-7. arXiv: hep-ex/0305031 [hep-ex].

[78] P. Abreu et al. "Search for stable heavy charged particles in e+ e- collisions at s**(1/2) = 130-GeV to 136-GeV, 161-GeV and 172-GeV". In: *Phys. Lett.* B396 (1997), pages 315–326. DOI: 10.1016/S0370-2693(97)00152-4.

[79] R. Akers et al. "Search for heavy charged particles and for particles with anomalous charge in e^+e^- collisions at LEP". In: *Z. Phys.* C67 (1995), pages 203–212. DOI: 10.1007/BF01571281.

[80] D. Buskulic et al. "Search for particles with unexpected mass and charge in Z decays". In: *Phys. Lett.* B303 (1993), pages 198–208. DOI: 10.1016/0370-2693(93)90066-Q.

[81] M. Banner et al. "A New Search for Relativistic Particles With Fractional Electric Charge at the CERN $p\bar{p}$ Collider". In: *Phys. Lett.* 156B (1985), pages 129–133. DOI: 10.1016/0370-2693(85)91368-1.

[82] F. Abe et al. "Limits on the production of massive stable charged particles". In: *Phys. Rev.* D46 (1992), R1889–R1894. DOI: 10.1103/PhysRevD.46.R1889.

[83] D. Acosta et al. "Search for long-lived charged massive particles in $\bar{p}p$ collisions at $\sqrt{s} = 1.8$ TeV". In: *Phys. Rev. Lett.* 90 (2003), page 131801. DOI: 10.1103/PhysRevLett.90.131801. arXiv: hep-ex/0211064 [hep-ex].

[84] Serguei Chatrchyan et al. "Search for fractionally charged particles in pp collisions at $\sqrt{s} = 7$ TeV". In: *Phys. Rev.* D87.9 (2013), page 092008. DOI: 10.1103/PhysRevD.87.092008. arXiv: 1210.2311 [hep-ex].

[85] M. Mori et al. "Search for fractionally charged particles in Kamiokande-II". In: *Phys. Rev.* D43 (1991), pages 2843–2846. DOI: 10.1103/PhysRevD.43.2843.

[86] M. Ambrosio et al. "Final search for lightly ionizing particles with the MACRO detector". In: (2004). arXiv: hep-ex/0402006 [hep-ex].

[87] Thomas K. Gaisser, Ralph Engel, and Elisa Resconi. *Cosmic Rays and Particle Physics*. Cambridge University Press, 2016. ISBN: 9780521016469, 9781316598917. URL: http://www.cambridge.org/de/academic/subjects/physics/cosmology-relativity-and-gravitation/cosmic-rays-and-particle-physics-2nd-edition?format=HB.

[88] The Nobel Prize. URL: https://www.nobelprize.org/prizes/physics/1936/ceremony-speech/.

[89] R. A. Millikan and G. H. Cameron. "The Origin of the Cosmic Rays". In: *Phys. Rev.* 32 (4 Oct. 1928), pages 533–557. DOI: 10.1103/PhysRev.32.533. URL: https://link.aps.org/doi/10.1103/PhysRev.32.533.

[90] J. Clay. *Penetrating radiation.* Volume 30. 1927, pages 1115–1127.

[91] M.H. Israel et al. "Isotopic Composition of Cosmic Rays: Results from the Cosmic Ray Isotope Spectrometer on the ACE Spacecraft". In: *Nuclear Physics A* 758 (2005). Nuclei in the Cosmos VIII, pages 201–208. ISSN: 0375-9474. DOI: https://doi.org/10.1016/j.nuclphysa.2005.05.038. URL: http://www.sciencedirect.com/science/article/pii/S037594740500686X.

[92] Pasquale Blasi. "The Origin of Galactic Cosmic Rays". In: *Astron. Astrophys. Rev.* 21 (2013), page 70. DOI: 10.1007/s00159-013-0070-7. arXiv: 1311.7346 [astro-ph.HE].

[93] Thomas K. Gaisser, Todor Stanev, and Serap Tilav. "Cosmic Ray Energy Spectrum from Measurements of Air Showers". In: *Front. Phys.(Beijing)* 8 (2013), pages 748–758. DOI: 10.1007/s11467-013-0319-7. arXiv: 1303.3565 [astro-ph.HE] (cited on pages 8, 9, 11).

[94] M A Malkov and L O'C Drury. "Nonlinear theory of diffusive acceleration of particles by shock waves". In: *Reports on Progress in Physics* 64.4 (2001), page 429. URL: http://stacks.iop.org/0034-4885/64/i=4/a=201.

[95] "Detection of the Small Magellanic Cloud in gamma-rays with Fermi/LAT". In: *Astron. Astrophys.* 523 (2010), A46. DOI: 10.1051/0004-6361/201014855. arXiv: 1008.2127 [astro-ph.HE].

[96] W. D. Apel et al. "Kneelike structure in the spectrum of the heavy component of cosmic rays observed with KASCADE-Grande". In: *Phys. Rev. Lett.* 107 (2011), page 171104. DOI: 10.1103/PhysRevLett.107.171104. arXiv: 1107.5885 [astro-ph.HE].

[97] A. P. Garyaka et al. "All-particle primary energy spectrum in the 3-200 PeV energy range". In: *J. Phys.* G35 (2008), page 115201. DOI: 10.1088/0954-3899/35/11/115201. arXiv: 0808.1421 [astro-ph].

[98] Kenneth Greisen. "End to the cosmic ray spectrum?" In: *Phys. Rev. Lett.* 16 (1966), pages 748–750. DOI: 10.1103/PhysRevLett.16.748.

[99] G. T. Zatsepin and V. A. Kuzmin. "Upper limit of the spectrum of cosmic rays". In: *JETP Lett.* 4 (1966). [Pisma Zh. Eksp. Teor. Fiz.4,114(1966)], pages 78–80.

[100] J. Bellido et al. "Proceedings of Science". In: *ICRC* 301 (506 2017).

[101] Alexander Aab et al. "Observation of a Large-scale Anisotropy in the Arrival Directions of Cosmic Rays above 8×10^{18} eV". In: *Science* 357.6537 (2017), pages 1266–1270. DOI: 10.1126/science.aan4338. arXiv: 1709.07321 [astro-ph.HE].

[102] E. Waxman. "IceCube's Neutrinos: The beginning of extra-Galactic neutrino astrophysics?" In: *Proceedings, 9th Rencontres du Vietnam: Windows on the Universe: Quy Nhon, Vietnam, August 11-17, 2013.* 2013, pages 161–168. arXiv: 1312.0558 [astro-ph.HE].

[103] A. M. Hillas. "The Origin of Ultrahigh-Energy Cosmic Rays". In: *Ann. Rev. Astron. Astrophys.* 22 (1984), pages 425–444. DOI: 10.1146/annurev.aa.22.090184.002233.

[104] Pablo M. Bauleo and Julio Rodriguez Martino. "The dawn of the particle astronomy era in ultra-high-energy cosmic rays". In: *Nature* 458N7240 (2009), pages 847–851. DOI: 10.1038/nature07948.

[105] P. O. Lagage and C. J. Cesarsky. "The maximum energy of cosmic rays accelerated by supernova shocks". In: *Astron. Astrophys.* 125 (1983), pages 249–257.

[106] T. Stanev. *High Energy Cosmic Rays.* Springer Praxis Books. Springer Berlin Heidelberg, 2010. ISBN: 9783540851486. URL: https://books.google.be/books?id=1y9YEYHAfBMC.

[107] C. Megan Urry and Paolo Padovani. "Unified schemes for radio-loud active galactic nuclei". In: *Publ. Astron. Soc. Pac.* 107 (1995), page 803. DOI: 10.1086/133630. arXiv: astro-ph/9506063 [astro-ph].

[108] Robert Antonucci. "Unified models for active galactic nuclei and quasars". In: *Ann. Rev. Astron. Astrophys.* 31 (1993), pages 473–521. DOI: 10.1146/annurev.aa.31.090193.002353.

[109] Demosthenes Kazanas et al. "Toward a Unified AGN Structure". In: (2012). arXiv: 1206.5022 [astro-ph.HE].

[110] J. Abraham et al. "Correlation of the highest-energy cosmic rays with the positions of nearby active galactic nuclei". In: *Astropart. Phys.* 29 (2008). [Erratum: Astropart. Phys.30,45(2008)], pages 188–204. DOI: 10.1016/j.astropartphys.2008.06.004,10.1016/j.astropartphys.2008.01.002. arXiv: 0712.2843 [astro-ph].

[111] M. G. Aartsen et al. "Multimessenger observations of a flaring blazar coincident with high-energy neutrino IceCube-170922A". In: *Science* 361.6398 (2018), eaat1378. DOI: 10.1126/science.aat1378. arXiv: 1807.08816 [astro-ph.HE].

[112] Ray W. Klebesadel, Ian B. Strong, and Roy A. Olson. "Observations of Gamma-Ray Bursts of Cosmic Origin". In: *Astrophys. J.* 182 (1973), pages L85–L88. DOI: 10.1086/181225.

[113] C. A. Meegan et al. "Spatial distribution of gamma-ray bursts observed by BATSE". In: *Nature* 355 (1992), pages 143–145. DOI: 10.1038/355143a0.

[114] Tsvi Piran. "The physics of gamma-ray bursts". In: *Rev. Mod. Phys.* 76 (2004), pages 1143–1210. DOI: 10.1103/RevModPhys.76.1143. arXiv: astro-ph/0405503 [astro-ph].

[115] B. P. Abbott et al. "GW170817: Observation of Gravitational Waves from a Binary Neutron Star Inspiral". In: *Phys. Rev. Lett.* 119.16 (2017), page 161101. DOI: 10.1103/PhysRevLett.119.161101. arXiv: 1710.05832 [gr-qc].

[116] B. P. Abbott et al. "GW170814: A Three-Detector Observation of Gravitational Waves from a Binary Black Hole Coalescence". In: *Phys. Rev. Lett.* 119.14 (2017), page 141101. DOI: 10.1103/PhysRevLett.119.141101. arXiv: 1709.09660 [gr-qc].

[117] B.. P.. Abbott et al. "GW170608: Observation of a 19-solar-mass Binary Black Hole Coalescence". In: *Astrophys. J.* 851.2 (2017), page L35. DOI: 10.3847/2041-8213/aa9f0c. arXiv: 1711.05578 [astro-ph.HE].

[118] Benjamin P. Abbott et al. "GW170104: Observation of a 50-Solar-Mass Binary Black Hole Coalescence at Redshift 0.2". In: *Phys. Rev. Lett.* 118.22 (2017). [Erratum: Phys. Rev. Lett.121,no.12,129901(2018)], page 221101. DOI: 10.1103/PhysRevLett.118.221101,10.1103/PhysRevLett.121.129901. arXiv: 1706.01812 [gr-qc].

[119] B. P. Abbott et al. "GW151226: Observation of Gravitational Waves from a 22-Solar-Mass Binary Black Hole Coalescence". In: *Phys. Rev. Lett.* 116.24 (2016), page 241103. DOI: 10.1103/PhysRevLett.116.241103. arXiv: 1606.04855 [gr-qc].

[120] F. Acero. "Detection of Gamma Rays From a Starburst Galaxy". In: *Science* 326 (2009), page 1080. DOI: 10.1126/science.1178826. arXiv: 0909.4651 [astro-ph.HE].

[121] Niklas Karlsson. "Discovery of VHE Gamma-ray Emission from the Starburst Galaxy M82". In: (2009). arXiv: 0912.3807 [astro-ph.HE].

[122] Kohta Murase, Susumu Inoue, and Shigehiro Nagataki. "Cosmic Rays above the Second Knee from Clusters of Galaxies and Associated High-Energy Neutrino Emission". In: *The Astrophysical Journal Letters* 689.2 (2008), page L105. URL: http://stacks.iop.org/1538-4357/689/i=2/a=L105.

[123] U. F. Katz and Ch. Spiering. "High-Energy Neutrino Astrophysics: Status and Perspectives". In: *Prog. Part. Nucl. Phys.* 67 (2012), pages 651–704. DOI: 10.1016/j.ppnp.2011.12.001. arXiv: 1111.0507 [astro-ph.HE].

[124] Morihiro Honda et al. "Calculation of atmospheric neutrino flux using the interaction model calibrated with atmospheric muon data". In: *Phys. Rev.* D75 (2007), page 043006. DOI: 10.1103/PhysRevD.75.043006. arXiv: astro-ph/0611418 [astro-ph] (cited on pages 9–11).

[125] M. G. Aartsen et al. "The IceCube Neutrino Observatory - Contributions to ICRC 2017 Part II: Properties of the Atmospheric and Astrophysical Neutrino Flux". In: (2017). arXiv: 1710.01191 [astro-ph.HE].

[126] Kiyoshi Niu, Eiko Mikumo, and Yasuko Maeda. "A Possible Decay in Flight of a New Type Particle". In: *Progress of Theoretical Physics* 46.5 (1971), pages 1644–1646. DOI: 10.1143/PTP.46.1644. eprint: /oup/backfile/content_public/journal/ptp/46/5/10.1143/ptp.46.1644/2/46-5-1644.pdf. URL: http://dx.doi.org/10.1143/PTP.46.1644.

[127] Rikard Enberg, Mary Hall Reno, and Ina Sarcevic. "Prompt neutrino fluxes from atmospheric charm". In: *Phys. Rev.* D78 (2008), page 043005. DOI: 10.1103/PhysRevD.78.043005. arXiv: 0806.0418 [hep-ph] (cited on pages 9–11).

[128] Linyan Wan et al. "Geoneutrinos at Jinping: Flux prediction and oscillation analysis". In: *Phys. Rev.* D95.5 (2017), page 053001. DOI: 10.1103/PhysRevD.95.053001. arXiv: 1612.00133 [hep-ex].

[129] Kate Scholberg. "Supernova Neutrino Detection". In: *Ann. Rev. Nucl. Part. Sci.* 62 (2012), pages 81–103. DOI: 10.1146/annurev-nucl-102711-095006. arXiv: 1205.6003 [astro-ph.IM].

[130] Lutz Kopke. "Supernova Neutrino Detection with IceCube". In: *J. Phys. Conf. Ser.* 309 (2011), page 012029. DOI: 10.1088/1742-6596/309/1/012029. arXiv: 1106.6225 [astro-ph.HE].

[131] C. Grupen. *Astroparticle physics.* 2005. ISBN: 9783540253129. URL: http://www.springer.com/book/3-540-25312-2.

[132] nobel1958. URL: https://www.nobelprize.org/prizes/physics/1958/summary/.

[133] "Design, Implementation and Test of a New Feature Extractor for the IceCube Neutrino Observatory". In: (2010).

[134] Dmitry Chirkin and Wolfgang Rhode. "Muon Monte Carlo: A High-precision tool for muon propagation through matter". In: (2004). arXiv: hep-ph/0407075 [hep-ph].

[135] D Schultz. "IceProd 2: A Next Generation Data Analysis Framework for the IceCube Neutrino Observatory". In: *Journal of Physics: Conference Series* 664.6 (2015), page 062056. URL: http://stacks.iop.org/1742-6596/664/i=6/a=062056 (cited on page 7).

[136] Giuseppe Battistoni et al. "Overview of the FLUKA code". In: *Annals Nucl. Energy* 82 (2015), pages 10–18. DOI: 10.1016/j.anucene.2014.11.007 (cited on page 9).

[137] Ralph Engel et al. "Towards the next generation of CORSIKA: A framework for the simulation of particle cascades in astroparticle physics". In: (2018). arXiv: 1808.08226 [astro-ph.IM] (cited on page 9).

[138] Askhat Gazizov and Marek P. Kowalski. "ANIS: High energy neutrino generator for neutrino telescopes". In: *Comput. Phys. Commun.* 172 (2005), pages 203–213. DOI: 10.1016/j.cpc.2005.03.113. arXiv: astro-ph/0406439 [astro-ph] (cited on page 9).

[139] M. G. Aartsen et al. "Observation of High-Energy Astrophysical Neutrinos in Three Years of IceCube Data". In: *Phys. Rev. Lett.* 113 (2014), page 101101. DOI: 10.1103/PhysRevLett.113.101101. arXiv: 1405.5303 [astro-ph.HE] (cited on pages 9–11).

[140] C. Andreopoulos et al. "The GENIE Neutrino Monte Carlo Generator". In: *Nucl. Instrum. Meth.* A614 (2010), pages 87–104. DOI: 10.1016/j.nima.2009.12.009. arXiv: 0905.2517 [hep-ph] (cited on page 10).

[141] Costas Andreopoulos et al. "The GENIE Neutrino Monte Carlo Generator: Physics and User Manual". In: (2015). arXiv: 1510.05494 [hep-ph] (cited on page 10).

[142] Mario Dunsch et al. "Recent Improvements for the Lepton Propagator PROPOSAL". In: (2018). arXiv: 1809.07740 [hep-ph] (cited on pages 12, 13).

[143] Dmitry Chirkin. “Study of South Pole ice transparency with IceCube flashers”. In: *Proceedings, 32nd International Cosmic Ray Conference (ICRC 2011): Beijing, China, August 11-18, 2011*. Volume 4, page 161. DOI: 10.7529/ICRC2011/V04/0333 (cited on page 14).

[144] Johan Lundberg et al. “Light tracking for glaciers and oceans: Scattering and absorption in heterogeneous media with Photonics”. In: *Nucl. Instrum. Meth.* A581 (2007), pages 619–631. DOI: 10.1016/j.nima.2007.07.143. arXiv: astro-ph/0702108 [ASTRO-PH] (cited on page 14).

Index

Corollaries, 33

Definitions, 33

Examples, 34
- Equation and Text, 34
- Paragraph of Text, 34

Exercises, 34

MMC, 14

PPC, 13

Problems, 34

PROPOSAL, 14

Propositions, 33
- Several Equations, 34
- Single Line, 34

Remarks, 33

Vocabulary, 34